Transverse Impact Simulation of CFRP Panels Using a Continuum Damage Mechanics Model in LS-DYNA

Scott J. Nesbitt, Sahar Abouali, Johannes Reiner*, Anoush Poursartip, Reza Vaziri
Composites Research Network; The University of British Columbia
*School of Engineering; Faculty of Science, Engineering and Built Environment; Deakin University
Vancouver, Canada; *Geelong, Australia

ABSTRACT

Impact damage prediction of non-crimp fabric CFRP panels is an area of interest for both automotive and aeronautical manufacturers. The University of British Columbia has been developing models to predict damage in composite materials since the mid 1990's [1]–[3] and has had the CODAM2 model implemented as MAT219 in the commercial FE program LS-DYNA since 2011.

In this paper, an end-to-end view is given of how to characterize composite materials to provide the inputs necessary for modelling with CODAM2 and the cohesive zone method. This includes an overview of the necessary test methods, post-test calibration procedures of the model, and subsequent application of the model to transverse impact simulations of a non-crimp fabric CFRP plate.

The results from the simulations are compared with experimental data [4], [5] in order to demonstrate the effectiveness of the model and provide insight into where further improvements can be made in modelling technology.

Corresponding author: Reza Vaziri – reza@composites.ubc.ca

1. INTRODUCTION

The second implementation UBC Composite Damage Model CODAM2 is a transversely isotropic continuum damage mechanics model based on a strain softening approach to predict the intra-laminar response of composite materials in finite element (FE) simulations. It is considered an elastic damage model and includes the capability for non-local damage implementation in order to eliminate mesh dependencies (element size and orientation) on the predicted size and direction of damage propagation. When combined with the cohesive zone method to model delamination, it forms a capable modelling tool for transverse impact simulation.

As with all damage models for orthotropic composite materials, several material parameters must be entered to fully describe the material. These include elastic constants, damage initiation values (strain for CODAM2 and peak stress/traction for cohesive zones), and fracture energy measures (provided as damage saturation strain values in CODAM2 and fracture energy for cohesive zones). By utilizing standard and non-standard test methods and applying the obtained values to an FE model of a transversely impacted composite plate, a method of determining the structural response of the plate and final damage state is developed. This paper provides an end-to-end discussion of how the inputs for this model are determined and implemented for transverse impact simulation. The outcome is then compared to experimental results.

In this paper, the conventions for principal material directions within the CODAM2 model in LS-DYNA are used. This consists of A (in-plane primary axis), B (in-plane transverse axis) and C (out-of-plane transverse axis). These are equivalent to the customary x, y, z or, – for unidirectional lamina – 1 (fiber axis), 2, 3 directions.

2. MATERIAL CHARACTERIZATION & IMPACT TEST DESCRIPTION

The material used in this work is a warp-knitted multiaxial non-crimp fabric (NCF) with a $[0_2/60/\text{-}60]_{2S}$ layup and therefore the properties of the laminate are not quasi-isotropic. The stitching was done at the sub-laminate level $[0_2/60/\text{-}60]$; therefore, the stitches do not provide any continuous through-thickness reinforcement other than at the sub-laminate level. The samples have an average tow width of 5 mm (as measured from stitch to stitch) and an average thickness of 2.56 mm. The fiber volume fraction is estimated to be between 0.45 and 0.50 based on optical micrographs, and the density was measured as 1523 kg/m^3 with ASTM D792 [6]. Impact samples were cut to be 100 mm x 100 mm in planar size and were impacted with 12.7 mm diameter spherical impactors having varying masses and energies. Details of the experimental work are not provided here, but can be found in [4] and [5].

3. CHARACTERIZATION OF INTRA-LAMINAR PROPERTIES

Standard Tests

3.1 Tensile Testing

Tensile testing is the most common material characterization test. Therefore, it will not be covered in great deal here except to say that obtaining actual in-situ strengths and fracture strains is difficult at best. Challenges of this test have been highlighted by numerous testing experts [7], [8] and often relate to challenges with gripping the sample to induce sufficiently high loads, or issues with elastic constraint in the transverse direction leading to matrix damage and splitting. The test is covered in ASTM D 3039 [9]. For the CODAM2 model the most important parameters are the tensile moduli and tensile damage initiation strains in both in-plane directions, as well as the in-plane Poisson’s ratio.

3.2 Compression Testing

While the CODAM2 model assumes that the elastic modulus in tension and compression modes of loading are identical, it does include mode specific damage initiation strains. These values are commonly produced in methods such as the IITRI method [10], and the more convenient combined loading compression method [11]. When tested, it is common that the elastic compressive modulus is lower than that of the elastic tensile modulus.

3.3 Flexural Testing

For models that are constructed using a sub-laminate or laminate method (i.e. the individual lamina are not resolved such that their orthotropic material properties and position in the thickness of the laminate are taken into account) a judgement must be made on using either the in-plane tensile/compressive modulus as measured above, or replacing these with the flexural modulus instead. For monolithic (non-layered) materials, the two properties are identical. Bending stiffness for both in-plane directions of the composite can be measured using 4-point bend tests and is covered in ASTM D7264 [12].

3.4 Intra-laminar Shear Testing

The number of shear property test methods is considerable and has been summarized succinctly in a column in CompositesWorld Magazine [13]; however, for intra-laminar shear properties the most common methods utilized include the Iosipescu (V-Notched Beam) method [14] and the V-Notched Rail Shear method [15], both of which have been compared and contrasted in another article [16].

The shear modulus is straightforward to attain from the strain gauges applied to the specimens and is the only shear property necessary for CODAM2. Enhancements to the CODAM2 model implemented as user subroutines – but not yet implemented directly in LS-DYNA – include the ability to model non-linear shear.

Non-Standard Tests

3.5 Intra-laminar Fracture Toughness

When composites fail in-plane, the total dissipated energy is higher than that represented by the area under the stress-strain curve of the linear loading region. Even for materials that appear to fail suddenly in a brittle fashion, there is energy that is dissipated post-peak in the creation of fracture surfaces, friction as material slides past each other, and to some extent plastic deformation in the polymer matrix. All these interacting failure modes serve to delay catastrophic failure by changing the notch-tip stress concentration within a fracture process zone (analogous to the plastic zone in metals) and redistributing stress to other regions. As elements in a simulation fail, it is important that a physically realistic amount of energy is absorbed. This is typically accomplished with a strain softening approach, where the stress-strain response after damage initiation results in a reduced elastic modulus for increasing strain as shown in Figure 1. The calibration of this strain-softening model is done through the characterization of intra-laminar fracture toughness which involves the use of tests like those found in fracture mechanics of metals. In the case of CODAM2 the actual model input is known as a damage saturation strain and is the strain value at which the material is fully damaged (secant modulus is zero). For CODAM2 in its local damage form, this can be readily calculated according to the formula:

$$\varepsilon_s = \frac{2g_c}{E\varepsilon_i} = \frac{2G_c}{EL_c\varepsilon_i} \qquad [1]$$

where the variables are as shown in Figure 1 and described below:
G_c = fracture toughness of the material (energy per unit area)

g_c = fracture energy density
L_c = characteristic length of the element
E = initial (undamaged) elastic modulus
ε_i = damage initiation strain

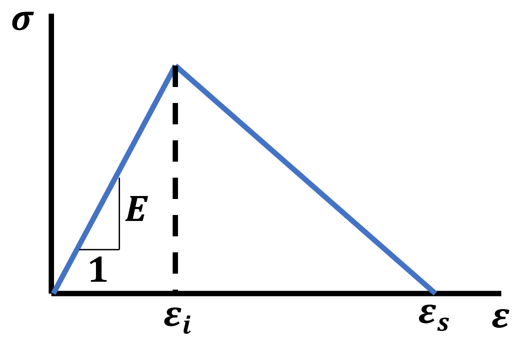

Figure 1. Bilinear stress-strain curve used in CODAM2

The characteristic length of the element is taken as the in-plane side length of a hex element and is used to convert the fracture toughness of the material (energy per area) into a fracture energy density (energy per volume) associated with an element of a given size. This is consistent with the crack band theory of Bazant [17] and ensures that the appropriate amount of energy is absorbed during failure of a given element size. Therefore, the fracture energy properties are a function of element size for the local method and make this method more suitable for implementation in models with elements of a constant size. The non-local method available in CODAM2 is not affected by this size dependency.

3.5.1 Intra-laminar Tensile Fracture Toughness

In the study of the fracture mechanics of metals, the use of compact tension specimens is common. Scaled up compact tension samples were made for plastic in ASTM D5014 [18]. Unfortunately, when scaled versions of this sample are applied to highly orthotropic composite samples, the response of the sample may not be as desired. Due to the orthotropic nature of the samples, damage can be initiated elsewhere outside of the intended fracture process zone. For this reason the over height compact tension specimen shown in Figure 2 and 3 was developed by Kongshavn and Poursartip [19]. The extended height increases the maximum load that the arms of the sample can sustain without damage. The oversized sample also ensures that there is sufficient linearly elastic material surrounding the propagating damage to ensure that linear elastic fracture mechanics is valid.

These samples are loaded quasi-statically under displacement control and may be stopped intermittently throughout the damage process to allow for ultrasonic c-scans to be made in order to characterize the size of the damage process zone during damage development. The height of the process zone is an important parameter for the calibration of non-local damage methods. It ensures that an accurate quantity of material around the simulated crack tip undergoes damage and provides a damage pattern that is not influenced by mesh orientation.

To determine the fracture toughness in both primary planar axes, tests must be conducted in two perpendicular directions to fully characterize the orthotropic specimen. In the case of the NCF material with a $[0_2/60/\text{-}60]_{2S}$ layup this corresponds to loading in the 0° direction (Case A) and loading in the 90° direction (Case B). The experimental results are shown in Figure 4.

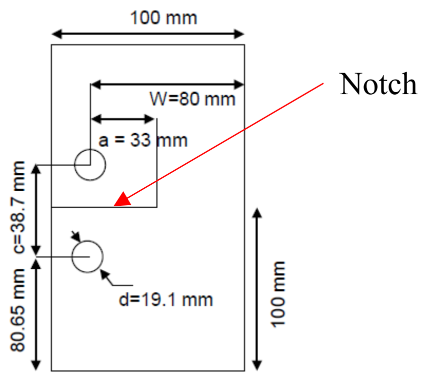

Figure 2. OCT specimen dimensions; the height is twice that of the width to ensure that damage initiates at the notch tip prior to the "arm" region

Figure 3. OCT specimen fixture configuration and loading direction; the metal bars clamped to the right side of the specimen limits out of plane bending

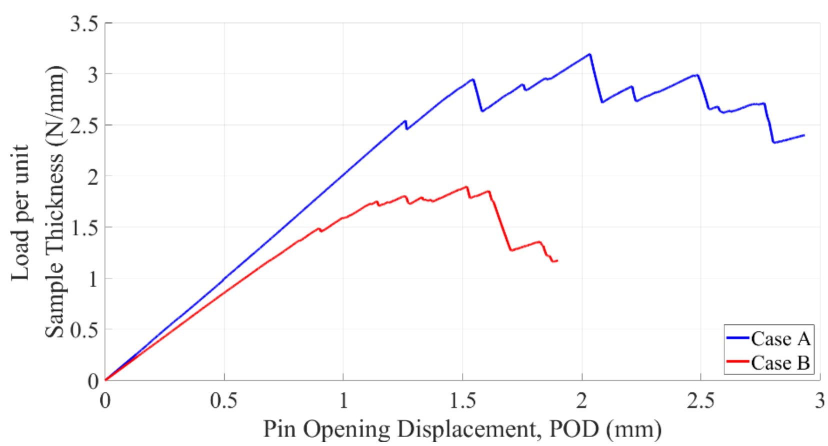

Figure 4. Load versus pin opening displacement of two OCT specimens showing the initial linear elastic response of the coupon followed by the progression of intra-laminar damage; Intra-laminar damage models should be calibrated in order to re-create similar load vs POD responses in a virtual test

To make this information useful for numerical analysis, an identical virtual test is often performed in order to calibrate the model to fit the observed experimental load-POD curve (inverse method); however, there are other methods involving non-contact strain field measurement (digital image correlation) in order to directly calculate the fracture energy values [20]. Methods such as these are only valid when the fracture process zone is visible from the exterior and therefore samples exhibiting substantial internal splitting and delamination must utilize the model calibration (inverse method). When the inverse method is used, the damage saturation strain value is found directly.

When modelling these virtual tests, care must be taken to ensure that the failure modes seen in the experiments are reproducible in the simulation. For example, Case B in Figure 4 exhibits damage due to self-similar crack growth largely as a result of matrix cracking and fiber breakage in the ±60° plies. This is seen in the ultrasonic inspection image of Figure 6 where the fracture process zone extends steadily towards the right (along the plane of the notch). In this case, the intra-laminar fracture of matrix and fiber is the dominant source of energy dissipation. With Case A the damage mode is not the same. In Figure 5 it is seen that there exists a large delamination zone extending perpendicular to the notch. This delamination is initiated by splitting that occurs in the matrix of the 0° lamina. Therefore, it is important that the model used to represent this material be capable of reproducing the interaction between matrix cracks and delamination initiation as an uncoupled model will not predict this delamination.

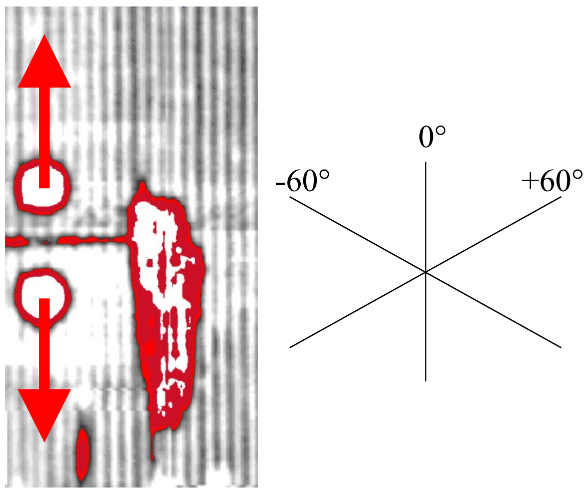

Figure 5. Ultrasonic inspection of Case A specimen; large region of splitting and non-self-similar matrix crack-initiated delamination is observed

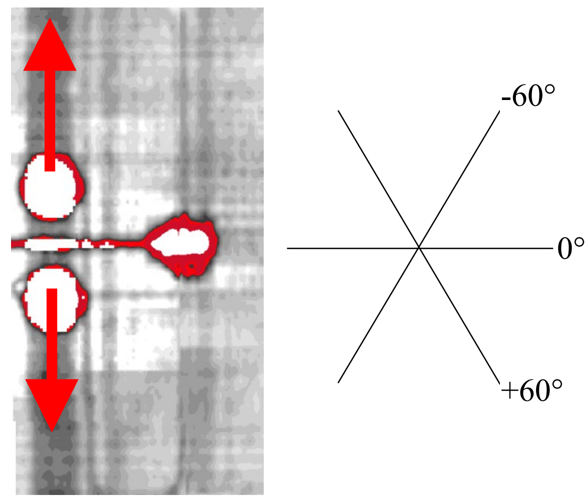

Figure 6. Ultrasonic Inspection of Case B specimen; self-similar crack growth consisting of matrix cracking and fiber breakage of the ±60° fibers is observed with minimal delamination

An example comparison of a virtual test with the experimental data is shown in Figure 7 below. The parameters of the virtual test (saturation strain in the fiber direction – and by extension, fracture toughness) are adjusted to achieve the best fit of data. The over-estimation of peak load in Figure 7 can be attributed to the lack of non-linear shear capability and the lack of interaction between matrix cracking and delamination initiation in this version of the model.

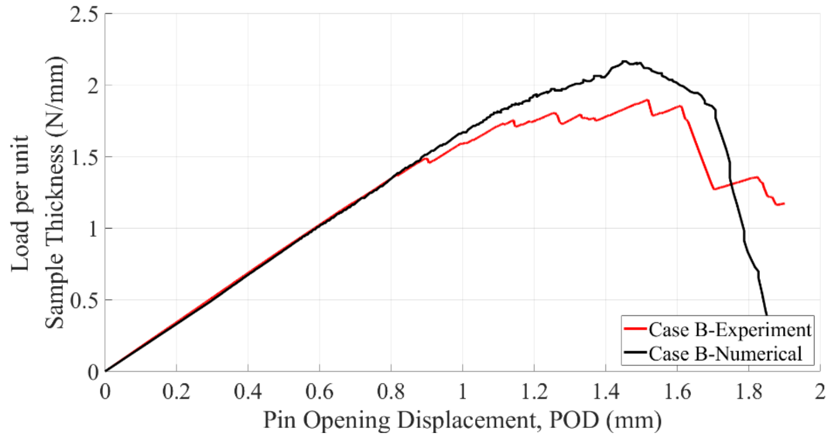

Figure 7. Load versus pin opening displacement of the Case B OCT specimen comparing experimental results with the numerical virtual test. The virtual test has been adjusted to best match the experimental response, thus calibrating the intra-laminar damage model

3.5.2 Intra-laminar Compression Fracture Toughness

Owing to the wide and varied damage modes present in composite materials, the intra-laminar fracture toughness of a laminate in compression is not the same as it is in tension. To characterize the intra-laminar fracture toughness in compression, a compact compression test is utilized. Under compression, it is known that kink band formation and widening is the primary damage mechanism for unidirectional composites, and in the case of a multidirectional laminate the effects of delamination and matrix cracking are also present. It is these different damage modes that result in the difference of fracture energies between tension and compression.

Due to kink band widening in the latter stages of compressive damage, the stress-strain response is known to contain a plateau region [21] as shown in Figure 8. CODAM2 does have the ability to account for this using the RESIDS parameter, However, in the current modelling of transverse impact we assume the simple bi-linear stress-strain response of Figure 1 in both tension and compression. A more independent material response has been implemented through user subroutines [22] and any future direct implementations of CODAM2 in LS-DYNA may feature this ability as well. If a plateau region is used in the stress-strain response, the non-contact method of fracture energy determination [20] provides a convenient method to optimize the shape of this response, but with additional effort the inverse method of model calibration can also work well.

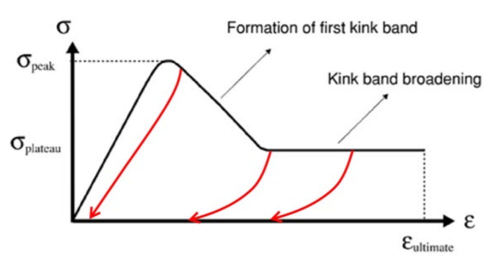

Figure 8. Compression-strain curve; kink band widening results in the plateau of stress at higher strains, giving a different strain softening response than that of tension shown in Figure 1

4. CHARACTERIZATION OF INTER-LAMINAR PROPERTIES

The inclusion of inter-laminar damage (commonly called delamination) is of critical importance for determining the structural response of a laminated composite, particularly for those that are transversely loaded and undergo substantial flexure. The orthotropic nature of composite lamina results in a mismatch of bending stiffness coefficients giving rise to substantial inter-laminar shear stress at the interfaces between layers. Delaminations in laminated composites can often extend much further beyond the typical intra-laminar damage region, particularly under high-velocity impact conditions [23]–[25].

4.1 Inter-laminar Tensile Testing (Mode I)

While CODAM2 only requires the transverse Poisson's ratio ν_{CB} – which may often reasonably be estimated from handbook values – the cohesive zone method does require a good estimate of the inter-laminar tensile strength to determine when delamination initiates in Mode I crack opening. In the tiebreak contact of LS-DYNA, this parameter is known as NFLS (normal failure stress) and a method to retrieve this value is covered in ASTM D7291 [26]. Through-thickness tensile modulus is not necessary for CODAM2 as it assumes transverse isotropy (which is applicable to unidirectionally reinforced composites) and this modulus is the same as E_B.

It should be noted that due to the finite size of an element being generally larger than the length scales at which fracture initiates, the interlaminar tensile strength from ASTM D7291 provides an upper limit of what should be used in the model. As element size increases, strength should be reduced to compensate for the inability to resolve localized high stress that causes initiation. Therefore, as an alternative to tests per ASTM D7291, a model with a certain mesh size can be calibrated using a virtual test of the end-notch flexure test covered in section 4.3.2 below. The inter-laminar strength is then adjusted until crack initiation occurs at the same load as the experiment.

4.2 Inter-laminar Shear Testing (Mode II)

While the V-notched rail shear or short beam shear test methods are applicable to determining inter-laminar shear properties (and preferable for modulus determination), the manufacture of their samples requires the production of at least 19 mm thick laminates for the V-Notched Beam method and 56 mm for the V-Notched Rail Shear method. At best this consumes a substantial amount of material, and at worst the extra thickness during processing results in a material that is not representative of the thinner laminate that may be used in the final product. For these reasons the short beam shear method described in ASTM D2344 [27] is commonly used. The method can characterize the inter-laminar shear strength required by the tiebreak contact of LS-DYNA (SFLS – shear failure strength); and the inter-laminar shear modulus is not required. The same comment on strength and element size as in the paragraph above also applies here, and calibration via a virtual test of the double-cantilever beam test may be used instead.

4.3 Inter-laminar Fracture Toughness

Just as an accurate value for intra-laminar fracture toughness was critical for determining the quantity of energy absorbed by the failing material under damage, so too is the inter-laminar fracture toughness for the interface. The two tests used for determining these material properties are described further below.

4.3.1 Mode I Inter-laminar Fracture Toughness

Mode I fracture is the smaller of the two most common modes (both in terms of fracture toughness value and in the amount of damage energy absorbed by this mode during an impact). This is generally due to the fact that impact produces through-thickness compressive stress waves which only become tensile once reflected from a free boundary. If these tensile stresses do cause delamination it is usually localized near the point of impact in thin samples because out of plane tensile stress cannot be sustained further away from the impact site owing to stress equilibrium. The exception being if substantial splitting occurs, thus making a layer more prone to delamination. Mode I fracture toughness for composite materials is found using the double cantilever beam test as outlined in ASTM D5528 [28]. A fully automated measurement of the Mode I fracture toughness has been recently developed in a modified double cantilever beam test using digital image correlation [29].

4.3.2 Mode II Inter-laminar Fracture Toughness

Mode II fracture is the dominant mode of delamination in composite panels under impact load. This is largely due to the orthotropic bending stiffness mismatch between adjacent layers, which under flexure gives rise to inter-laminar shear stresses [30]. Mode II fracture toughness for composite materials is found using the double cantilever beam test as outlined in ASTM D7905 [31].

5. NUMERICAL MODEL

Owing to the complexity of modelling composite materials (orthotropic nature, numerous interconnected failure modes, etc.) several methods have been proposed and developed to account for the nature of composite materials. Summaries of many of these methods can be found in various sources such as Comprehensive Composite Materials II [32], Numerical Modelling of Failure in Advanced Composites [33] and of course the World Wide Failure Exercises [34]. As discussed above, this paper focuses on the use of CODAM2 for the simulation of intra-laminar damage and the cohesive zone method for inter-laminar damage.

The model geometry is shown in Figure 9 and 10. It consists of a 100 mm x 100 mm x 2.56 mm composite part with several layers. This part is modelled with 1 mm square solid, constant stress (ELFORM 1) elements. Solid elements were chosen over shell elements to include through-thickness elastic displacements locally in the region of the impactor. This part is sitting on a support frame modelled as a rigid body with a 75 mm x 75 mm square cutout. The impactor is a 12.7 mm diameter hemisphere that is also modelled as a rigid body. Nodal constraints in the out-of-plane direction are applied in four locations where the sample is clamped during the experiments.

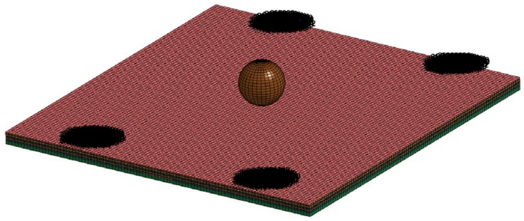

Figure 9. Overview of entire LS-DYNA Model domain; Impactor is the brown sphere; the black circular regions are nodal constraints to mimic the effect of the specimen clamps

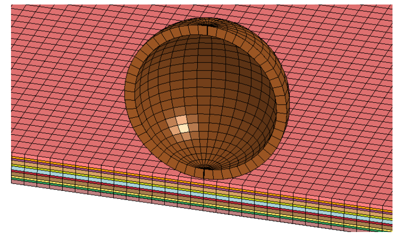

Figure 10. Closeup cross-section view near the impact site; the 11 layers of composite can be clearly seen; the spherical indenter is modelled as a rigid body and therefore the hollow geometry does not affect the results

5.1 Intra-laminar Model

The UBC CODAM2 model is available as a native material model (MAT219) in LS-DYNA. The CODAM model was originally developed by Williams, et. al. [1] and CODAM2 was developed later by Forghani, et. al. [35] to enable non-local methods of damage development.

For this work, the local version of MAT219 is used to predict the structural response and subsequent impact damage in transversely impacted NCF plates. It was found that for these transverse impacts on NCF material it was important to model the structure at the lamina level in order to account for the absorption of energy by inter-laminar delamination. This delamination is due to the high inter-laminar shear stress generated as a result of the flexure of the panels and their mismatch of bending stiffness between adjacent layers as discussed by Liu [30].

After carrying out material characterization tests on the NCF laminate, the elastic parameters for the individual lamina were back-calculated using classical laminate plate theory such that the re-produced laminate as a whole had the elastic properties measured in the material characterization tests. In-plane damage initiation strains are taken directly from laminate tensile test failure strains and in-plane saturation strains (fracture energies) are based on the inverse method described in section 3.5.1. The parameters used for the numerical model are shown in Table 1 below.

Table 1. Intra-laminar material parameters for LS-DYNA MAT219 impact model

ρ (g/mm^3)	E_A (MPa)	E_B (MPa)	ν_{BA} (-)	ν_{CB} (-)	G_{AB} (MPa)	Initiation Strain (-)				Fracture Energy (kJ/m^2)	
						Matrix		Fiber		Matrix	Fiber
						Tens.	Comp.	Tens.	Comp.		
0.001523	116000	14000	0.03	0.5	3000	0.0046	0.0150	0.0157	0.0160	3.5	95

5.2 Inter-laminar Model

Automatic One-Way Surface-to-Surface Tiebreak contacts are used to model the interface between adjacent layers of the laminate. Option 9 is selected, which corresponds to a model that is based on the MAT138 cohesive element and accounts for mixed mode delamination. This model requires the specification of the peak normal traction (inter-laminar tensile strength) and peak shear traction (inter-laminar shear strength) to determine the onset of damage coupled with the inter-laminar fracture toughness for Mode I and Mode II (G_{IC} & G_{IIC}). Like the strain-softening approach used in the intra-laminar model of CODAM2, the stiffness between nodes on either side of the interface is reduced as their separation is increased in a way that ensures the energy dissipation per unit area of interface is consistent with the fracture energy of the mode (mostly mode II) causing the delamination. The parameters used for the numerical model are shown in Table 2 below.

Table 2. Inter-laminar material parameters for LS-DYNA MAT219 impact model

Inter-laminar Tensile Strength (MPa)	**Inter-laminar Shear Strength (MPa)**	**Mode I Fracture Energy (kJ/m^2)**	**Mode II Fracture Energy (kJ/m^2)**
60.0	63.6	0.49	1.80

6. RESULTS

The model was tested with three different impactor masses at various impact velocities, resulting in numerous impact energies. The following results show an example for a drop eight impact test with a mass of 2818 g and an impact velocity of 2.70 m/s, giving an impact energy of 10.3 J or 4.0 J per millimeter of sample thickness. The predicted force versus displacement response is shown in Figure 11 in comparison with the experimental impact and quasistatic loading results. It can be seen that this impact is representative of a low-velocity impact by virtue of the response closely following that of the quasistatic test. Furthermore, the model is capable of accurately predicting the loading response of the sample, but is seen to give a slightly higher peak load (4750 N vs. 4600 N) and slightly lower peak displacement (4.43 mm vs. 4.69 mm) indicating some lack of energy absorbance.

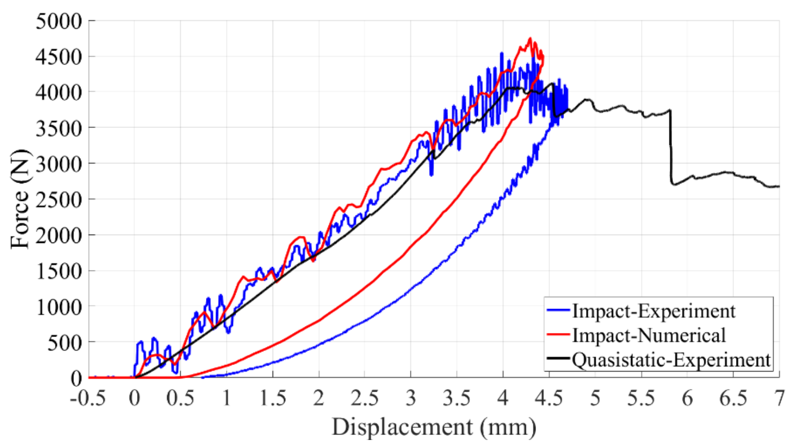

Figure 11. Comparison of force versus displacement curves between the numerical impact simulation and experimental drop tower impact of 10.3 J with an impact velocity of 2.70 m/s; results agree closely and almost overlap the curve corresponding to the quasistatic experiment

This discrepancy can be attributed to the inability of the model to accurately capture the splitting and tow delamination phenomenon observed in the experiment as shown in Figure 12 below. In this figure it can be seen that two tows have nearly completely delaminated from the coupon. It is believed that the effect of the warp direction stitches on the surface of the laminate contribute towards this failure mode as they interrupt the load path between adjacent tows, making splitting more likely to occur. It can be seen in Figure 12c that the model does not predict this region of damage, and therefore the peak load is higher than expected and the maximum deformation of the plate slightly lower.

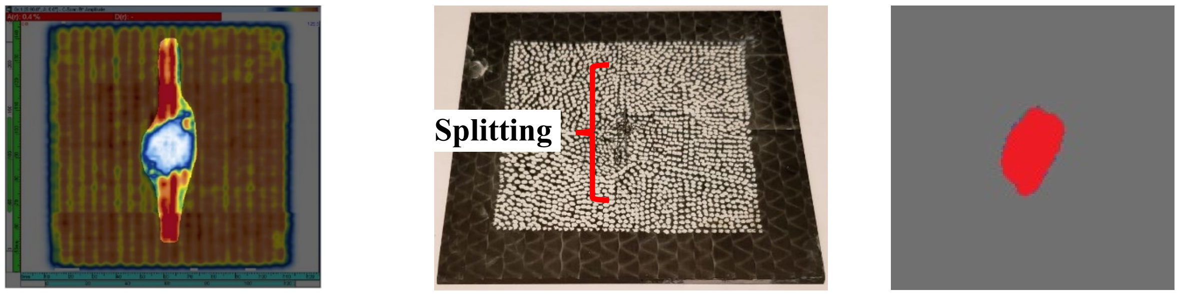

(a) **(b)** **(c)**

Figure 12. Delamination damage observed in experiments (a) and (b), and in the numerical model (c); the numerical model correctly predicts delamination below the impact site, but does not account for mesoscopic delamination associated with substantial tow delamination delineated by the NCF stitching

7. CONCLUSIONS

An end-to-end view of the material characterization tests and calibration procedures for orthotropic composite damage models has been described with specific emphasis on characterization for use in the UBC CODAM2 damage model. This included volumetric tests (density), intra-laminar tests and inter-laminar tests to fully characterize the material. These material values were then applied to a numerical model utilizing the LS-DYNA built-in MAT219 representation of the CODAM2 intra-laminar damage model capable of modelling a transversely isotropic elastic material. Inter-laminar damage was modelled with the use of the tiebreak contact in a similar fashion to that of the MAT138 mixed mode cohesive zone element. The structural response obtained from impact simulations were found to be very close to that measured from impact experiments, but slightly too stiff, possibly owing to the inability of the model to accurately capture the matrix splitting effect seen in the experiment. The model shows good promise for predicting damage in transverse impact cases, but additional refinement to include the effect of splitting in surface layers (aided by NCF stitching) would provide additional improvements to the model.

8. REFERENCES

[1] K. V. Williams, R. Vaziri, and A. Poursartip, “A physically based continuum damage mechanics model for thin laminated composite structures,” *Int. J. Solids Struct.*, vol. 40, no. 9, pp. 2267–2300, May 2003, doi: 10.1016/S0020-7683(03)00016-7.

[2] A. Forghani, A. Poursartip, and R. Vaziri, “An orthotropic non-local approach to modeling intra-laminar damage progression in laminated composites,” *Int. J. Solids Struct.*, vol. 180–181, pp. 160–175, Dec. 2019, doi: 10.1016/J.IJSOLSTR.2019.07.015.

[3] M. Shahbazi, “An efficient virtual testing framework to simulate the progression of damage in notched composite laminates,” The University of British Columbia, 2017, doi: 10.14288/1.0354263.

[4] S. Nesbitt, R. Vaziri, and A. Poursartip, “Characterization of the Structural Response and Energy Absorption Characteristics of Braided and Non-Crimp Fabric CFRP Panels Subjected to Transverse Impact Loadings at Variable Strain Rates,” in *4th International Aerospace Structural Impact Dynamics Conference*, 2019.

[5] S. Nesbitt, M. Waimer, N. Toso-Pentecôte, R. Vaziri, and A. Poursartip, “Structural Response and Damage Characterisation of Non-Crimp Fabric CFRP Panels under Impact Loading,” in *11th Canadian-International Conference on Composites*, 2019.

[6] “D792-13 Standard Test Methods for Density and Specific Gravity (Relative Density) of Plastics by Displacement.” ASTM International, West Conshohocken, PA, 2013, doi: https://doi.org/10.1520/D0792-13.

[7] D. Adams, “Unidirectional composite axial tensile specimens,” *CompositesWorld*, 2006. [Online]. Available: https://www.compositesworld.com/articles/unidirectional-composite-axial-tensile-specimens. [Accessed: 15-Jan-2020].

[8] D. Adams, “Composite material testing: How do I know if my measured composite properties are correct, or even reasonable?,” *CompositesWorld*, 2018. [Online]. Available: https://www.compositesworld.com/blog/post/how-do-i-know-if-my-measured-composite-properties-are-correct-or-even-reasonable. [Accessed: 15-Jan-2020].

[9] “D3039-17 Standard Test Method for Tensile Properties of Polymer Matrix Composite Materials.” ASTM International, West Conshohocken, PA, 2017, doi: https://doi.org/10.1520/D3039_D3039M-17.

[10] “D3410-16 Standard Test Method for Compressive Properties of Polymer Matrix Composite Materials with Unsupported Gage Section by Shear Loading.” ASTM International, West Conshohocken, PA, 2016, doi: https://doi.org/10.1520/D3410_D3410M-16.

[11] “D6641-16 Standard Test Method for Compressive Properties of Polymer Matrix Composite Materials Using a Combined Loading Compression (CLC) Test Fixture.” ASTM International, West Conshohocken, PA, 2016, doi: https://doi.org/10.1520/D6641_D6641M-16E01.

[12] “D7264-15 Standard Test Method for Flexural Properties of Polymer Matrix Composite Materials.” 2015, doi: https://doi.org/10.1520/D7264_D7264M-15.

[13] D. Adams, “A comparison of shear test methods,” *CompositesWorld*, 2009. [Online]. Available: https://www.compositesworld.com/articles/a-comparison-of-shear-test-methods. [Accessed: 14-Jan-2020].

[14] “D5379-12 Standard Test Method for Shear Properties of Composite Materials by the V-

Notched Beam Method." ASTM International, West Conshohocken, PA, 2012, doi: https://doi.org/10.1520/D5379_D5379M-19.

[15] "D7078-19 Standard Test Method for Shear Properties of Composite Materials by V-Notched Rail Shear Method." ASTM International, West Conshohocken, PA, 2019, doi: https://doi.org/10.1520/D7078_D7078M-19.

[16] D. Adams, "Shear test methods: Iosipescu vs. V-Notched Rail," *CompositesWorld*, 2009. [Online]. Available: https://www.compositesworld.com/articles/shear-test-methods-iosipescu-vs-v-notched-rail. [Accessed: 14-Jan-2020].

[17] Z. P. Bazant and J. Planas, *Fracture and Size Effect in Concrete and Other Quasibrittle Materials*. Boca Raton: CRC Press LLC, 1998.

[18] "D5045-14 Standard Test Methods for Plane-Strain Fracture Toughness and Strain Energy Release Rate of Plastic Materials." ASTM International, West Conshohocken, PA, 2014, doi: https://doi.org/10.1520/D5045-14.

[19] I. Kongshavn and A. Poursartip, "Experimental investigation of a strain-softening approach to predicting failure in notched fibre-reinforced composite laminates," *Compos. Sci. Technol.*, vol. 59, no. 1, pp. 29–40, Jan. 1999, doi: 10.1016/S0266-3538(98)00034-7.

[20] N. Zobeiry, R. Vaziri, and A. Poursartip, "Characterization of strain-softening behavior and failure mechanisms of composites under tension and compression," *Compos. Part A Appl. Sci. Manuf.*, vol. 68, pp. 29–41, Jan. 2015, doi: 10.1016/J.COMPOSITESA.2014.09.009.

[21] Y. Yuan, K. Niu, and Z. Zhang, "Compressive damage mode manipulation of fiber-reinforced polymer composites," *Eng. Fract. Mech.*, vol. 223, p. 106799, Jan. 2020, doi: 10.1016/J.ENGFRACMECH.2019.106799.

[22] J. Reiner and R. Vaziri, "Local and Nonlocal Continuum Damage Simulation of Impact and Compression After Impact Tests on CFRP Laminates," in *22nd International Conference on Composite Materials (ICCM22)*, 2019.

[23] R. Olsson, "Mass criterion for wave controlled impact response of composite plates," *Compos. Part A Appl. Sci. Manuf.*, vol. 31, no. 8, pp. 879–887, Aug. 2000, doi: 10.1016/S1359-835X(00)00020-8.

[24] W. J. Cantwell and J. Morton, "Comparison of the low and high velocity impact response of CFRP," *Composites*, vol. 20, no. 6, pp. 545–551, Nov. 1989, doi: 10.1016/0010-4361(89)90913-0.

[25] H. Morita, T. Adachi, Y. Tateishi, and H. Matsumot, "Characterization of Impact Damage Resistance of CF/PEEK and CF/Toughened Epoxy Laminates under Low and High Velocity Impact Tests," *J. Reinf. Plast. Compos.*, vol. 16, no. 2, pp. 131–143, Jan. 1997, doi: 10.1177/073168449701600203.

[26] "D7291-15 Standard Test Method for Through-Thickness 'Flatwise' Tensile Strength and

Elastic Modulus of a Fiber-Reinforced Polymer Matrix Composite Material.” ASTM, West Conshohocken, PA, 2015, doi: https://doi.org/10.1520/D7291_D7291M-15.

[27] “D2344-16 Standard Test Method for Short-Beam Strength of Polymer Matrix Composite Materials and Their Laminates.” ASTM International, West Conshohocken, PA, 2016, doi: https://doi.org/10.1520/D2344_D2344M-16.

[28] “D5528-13 Standard Test Method for Mode I Interlaminar Fracture Toughness of Unidirectional Fiber-Reinforced Polymer Matrix Composites BT - Standard Test Method for Mode I Interlaminar Fracture Toughness of Unidirectional Fiber-Reinforced Polymer Matrix.” ASTM International, West Conshohocken, PA, 2013, doi: https://doi.org/10.1520/D5528-13.

[29] J. Reiner, J. P. Torres, and M. Veidt, “A novel Top Surface Analysis method for Mode I interface characterisation using Digital Image Correlation,” *Eng. Fract. Mech.*, vol. 173, pp. 107–117, Mar. 2017, doi: 10.1016/J.ENGFRACMECH.2016.12.022.

[30] D. Liu, “Impact-Induced Delamination—A View of Bending Stiffness Mismatching,” *J. Compos. Mater.*, vol. 22, no. 7, pp. 674–692, Jul. 1988, doi: 10.1177/002199838802200706.

[31] “D7905-14 Standard Test Method for Determination of the Mode II Interlaminar Fracture Toughness of Unidirectional Fiber-Reinforced Polymer Matrix Composites BT - Standard Test Method for Determination of the Mode II Interlaminar Fracture Toughness of Uni.” ASTM International, West Conshohocken, PA, 2014, doi: https://doi.org/10.1520/D7905_D7905M-19E01.

[32] J. Reiner and R. Vaziri, “Structural Analysis of Composites With Finite Element Codes: An Overview of Commonly Used Computational Methods,” in *Comprehensive Composite Materials II*, vol. 8, P. W. R. Beaumont and C. H. Zweben, Eds. Elsevier Ltd., 2018, pp. 61–84.

[33] A. Forghani, M. Shahbazi, N. Zobeiry, A. Poursartip, and R. Vaziri, “An overview of continuum damage models used to simulate intralaminar failure mechanisms in advanced composite materials,” in *Numerical Modelling of Failure in Advanced Composite Materials*, P. P. Camanho and S. R. Hallett, Eds. Woodhead Publishing, 2015, pp. 151–173.

[34] A. S. Kaddour, M. J. Hinton, P. A. Smith, and S. Li, “The background to the third world-wide failure exercise,” *J. Compos. Mater.*, vol. 47, no. 20–21, pp. 2417–2426, Sep. 2013, doi: 10.1177/0021998313499475.

[35] A. Forghani, N. Zobeiry, A. Poursartip, and R. Vaziri, “A structural modelling framework for prediction of damage development and failure of composite laminates,” *J. Compos. Mater.*, vol. 47, no. 20–21, pp. 2553–2573, Sep. 2013, doi: 10.1177/0021998312474044.